Relaxin receptor antagonist AT-001 synergizes with docetaxel in androgen-independent prostate xenografts

Anton Neschadim, Laura B Pritzker[1], Kenneth P H Pritzker[1,2,3,4], Donald R Branch[5,6,7,8], Alastair J S Summerlee[9], John Trachtenberg[10,11,12,13] and Joshua D Silvertown

Armour Therapeutics, Inc., 124 Orchard View Boulevard, Toronto, Ontario, Canada
[1]Rna Diagnostics, Inc., 595 Bay Street, Suite 1204, Toronto, Ontario, Canada
Departments of [2]Laboratory Medicine and Pathobiology, and [3]Surgery, University of Toronto, Toronto, Ontario, Canada
[4]Pathology and Laboratory Medicine, Mount Sinai Hospital, Toronto, Ontario, Canada
Departments of [5]Medicine and [6]Laboratory Medicine and Pathobiology, University of Toronto, Toronto, Ontario, Canada
[7]Centre for Innovation, Canadian Blood Services, Toronto, Ontario, Canada
[8]Division of Advanced Diagnostics – Infection and Immunity, Toronto General Research Institute (TGRI), University Health Network, Toronto, Ontario, Canada
[9]Department of Biomedical Sciences, University of Guelph, Guelph, Ontario, Canada
[10]Departments of Surgery and Medical Imaging, University of Toronto, Toronto, Ontario, Canada
[11]Division of Urology, Department of Surgical Oncology, [12]Prostate Centre, Princess Margaret Hospital, and
[13]Ontario Cancer Institute, Princess Margaret Cancer Centre, University Health Network, Toronto, Ontario, Canada

Correspondence should be addressed to J D Silvertown
Email
josh@armourtherapeutics.com

Abstract

Androgen hormones and the androgen receptor (AR) pathway are the main targets of anti-hormonal therapies for prostate cancer. However, resistance inevitably develops to treatments aimed at the AR pathway resulting in androgen-independent or hormone-refractory prostate cancer (HRPC). Therefore, there is a significant unmet need for new, non-androgen anti-hormonal strategies for the management of prostate cancer. We demonstrate that a relaxin hormone receptor antagonist, AT-001, an analog of human H2 relaxin, represents a first-in-class anti-hormonal candidate treatment designed to significantly curtail the growth of androgen-independent human prostate tumor xenografts. Chemically synthesized AT-001, administered subcutaneously, suppressed PC3 xenograft growth by up to 60%. AT-001 also synergized with docetaxel, standard first-line chemotherapy for HRPC, to suppress tumor growth by more than 98% in PC3 xenografts via a mechanism involving the downregulation of hypoxia-inducible factor 1 alpha and the hypoxia-induced response. Our data support developing AT-001 for clinical use as an anti-relaxin hormonal therapy for advanced prostate cancer.

Key Words
- prostate cancer
- anti-hormone therapy
- angiogenesis
- relaxin
- relaxin antagonist
- androgen independence
- docetaxel
- tumor xenografts

Endocrine-Related Cancer (2014) **21**, 459–471

Introduction

Interfering with the androgen receptor (AR) pathway has been the main focus of therapeutic interventions in prostate cancer (Heinlein & Chang 2004). Despite recent advances in clinical development of second-generation anti-androgens, namely, cytochrome P450 17A1 (CYP17A1) inhibitors such as abiraterone acetate (Zytiga)

http://erc.endocrinology-journals.org
DOI: 10.1530/ERC-14-0088

Published by Bioscientifica Ltd.

and AR antagonists such as enzalutamide (Xtandi) and ARN-509 (currently in clinical development), resistance to these therapies still develops rapidly (Joseph *et al*. 2013, Korpal *et al*. 2013, Yuan *et al*. 2013). As the cancer progresses, there is a shift from androgen dependence to pathways that favor proliferation-, survival-, and angiogenesis-promoting signals, often in crosstalk with the AR pathway (Reis 2012). More than 40% of prostate cancer patients will develop hormone-refractory prostate cancer, with the average survival estimated at just 18 months (Gulley *et al*. 2003). Therefore, targeting other non-androgen pathways in advanced prostate cancer represents an unmet clinical need, and the relaxin hormone pathway is one such pathway that is implicated in the progression of advanced prostate cancer (Hombach-Klonisch *et al*. 2006, Feng *et al*. 2007).

Relaxin increases prostate tumor growth by virtue of its ability to induce cellular proliferation and increase tumoral blood vessels, which are critical for tumor growth and viability (Silvertown *et al*. 2003, Hombach-Klonisch *et al*. 2006, Feng *et al*. 2007). The role of relaxin in prostate cancer progression is increased upon transition to androgen independence. Three potential pathways may be involved: i) mutations in the tumor-suppressor gene *p53* (*TP53*), which facilitates androgen-independent tumor growth – the relaxin pathway has been implicated in driving this process (Thompson *et al*. 2006, Vinall *et al*. 2006); ii) relaxin stimulates cell proliferation, angiogenesis (via upregulation of VEGF), extracellular matrix remodeling, tumoral blood flow, and apoptosis (Silvertown *et al*. 2003, 2007, Hombach-Klonisch *et al*. 2006); and iii) relaxin can drive the activation of the AR signaling pathway via an intracellular mechanism that is independent of external stimulation by androgens. In the absence of androgen, relaxin promotes downstream AR signaling via crosstalk with the Wnt signaling pathway through the induction and stabilization of cytoplasmic β-catenin (Vinall *et al*. 2006, Liu *et al*. 2008). Therefore, blocking relaxin would engender a first-in-class anti-hormonal therapy with both anti-relaxin and anti-androgen functional characteristics. Besides a well-characterized role in prostate cancer, relaxin has also been implicated in a number of other human cancers, including breast (Tashima *et al*. 1994), thyroid (Hombach-Klonisch *et al*. 2006), endometrium (Kamat *et al*. 2006), as well as bone, liver, and esophagus.

We and others have shown that modification of the H2 relaxin hormone in its receptor-binding domain (RBD) renders it a receptor antagonist, thereby neutralizing endogenous H2 relaxin signaling (Silvertown *et al*. 2007, Hossain *et al*. 2010). We showed that recombinant human H2 relaxin receptor antagonist expressed from prostate cancer xenografts results in significantly impaired tumor growth (Silvertown *et al*. 2007). The current work describes the development and characterization of chemically synthesized AT-001, a relaxin receptor antagonist, and the effect of its systemic administration on the growth of aggressive, androgen-independent human prostate cancer tumor xenografts. We further show that AT-001 treatment synergistically combines with standard first-line chemotherapy, docetaxel (Garmey *et al*. 2008, Carles *et al*. 2012), and that hypoxia-induced response plays a key role in the underlying mechanism.

Subjects and methods

Cell culture and other reagents

Human prostatic adenocarcinoma PC3 (CRL-1435), human embryonic kidney 293 (HEK293) (CRL-1573), and the HEK293-derived 293T (CRL-3216) cell lines were obtained from the American Type Culture Collection (ATCC, Manassas, VA, USA) and cultured as described previously (Hombach-Klonisch *et al*. 2006). PC3 cell line was authenticated by STR profiling by The Centre for Applied Genomics (The Hospital for Sick Children, Toronto, ON, Canada) using the AmpFLSTR Identifier PCR Amplification Kit (Life Technologies) (Amelogenin: X; CSF1PO: 11; D13S317: 11; D16S539: 11; D18S51: 14,15; D19S433: 14; D21S11: 29,31.2; D2S1338: 18,20; D3S1358: 16; D5S818: 13; D7S820: 8; D8S1179: 13; FGA: 24; THO1: 6,7; and TPOX: 8,9; vWA: 17; 92% match with the ATCC STR Database). HEK293.RXFP1 and 293T.RXFP1 stably transfected cell lines were obtained from parental HEK293 and 293T cell lines, respectively, by transfection of the pCDNA3.1/Zeo-LGR7 (relaxin/insulin-like family peptide receptor 1 (RXFP1)) plasmid (Silvertown *et al*. 2006*a*). HEK293.RXFP1.mGL.2 (clone #1) cell line was derived by stable transfection of HEK293.RXFP1 cells with the pCRE-mGL.2 plasmid (Xactagen, Shoreline, WA, USA), carrying membrane-anchored Gaussia luciferase (Verhaegent & Christopoulos 2002) (see Supplementary Materials and Methods, see section on supplementary data given at the end of this article). Docetaxel (Cayman Chemical, Ann Arbour, MI, USA) was formulated in anhydrous ethanol, combined with polysorbate 80 to give a 50 mg/ml concentrated stock solution, and, before injection, diluted in 5% dextrose in water to a final concentration. Lyophilized H2 relaxin (Bachem, Torrance, CA, USA) and AT-001 were reconstituted in a 20 mM sodium acetate, pH

http://erc.endocrinology-journals.org
DOI: 10.1530/ERC-14-0088

Published by Bioscientifica Ltd.

5.0, buffer to yield 0.75 mg/ml stock solutions, and subsequently diluted before injection. AT-001 was synthesized by solid-phase peptide synthesis (see Supplementary Materials and Methods).

Receptor-binding bioassay: radioligand-binding assay

Radioactively labeled H2 relaxin was prepared by labeling the synthetic protein with the Pierce Iodination Reagent (1,3,4,6-tetrachloro-3α,6α-diphenyl-glycoluril; Pierce Iodination Tubes, Thermo Fisher Scientific, Rockford, IL, USA) following the manufacturer's instructions (see Supplementary Materials and Methods). Radioligand-binding assay (RBA) was performed to determine K_d and K_i binding constants for H2 relaxin and AT-001, respectively, as following: 10^5 293T.RXFP1 cells were seeded per well of a 24-well tissue culture plate and cultured overnight. Before the assay, culture media were removed, cells were washed with HEPES binding buffer (HBB, 100 mM NaCl, 5 mM KCl, 1.3 mM $MgSO_4$, 1 mM EDTA, 10 mM glucose, 15 mM NaOAc, 100 mM HEPES, 1% BSA, and pH 7.4), and replaced with warm HBB. ^{125}I-labeled H2 relaxin, and 'cold' H2 relaxin or AT-001 were added together at a range of concentrations and incubated for 2 h at room temperature. A saturating concentration of 'cold' H2 relaxin (500 nM) was utilized to evaluate non-specific binding. Following the incubation, cells were washed twice with HBB and lysed with 1 M NaOH for 30 min at room temperature. Lysates were collected and analyzed on a GammaMaster 1277 gamma counter (LKB, Wallac, Finland).

Relaxin bioactivity assay and competitive inhibition assay: Gaussia luciferase-based reporter assay

Stimulation of cAMP and competitive inhibition of H2 relaxin-mediated cAMP stimulation by AT-001 were assessed as following: 5×10^4 HEK293.RXFP1.mGL. Two cells were seeded per well of a 96-well tissue culture plate and cultured overnight. Media were changed 30 min before the addition of treatment samples. Pre-mixed, concentrated treatment samples were then added to each well to yield a final concentration of 50 μM 3-isobutyl-1-methylxanthine (IBMX), and the vehicle or desired treatment concentration of H2 relaxin, AT-001, or H2 relaxin and AT-001. All treatments were performed in at least duplicate. Following stimulation for 6 h at 37 °C in a humidified atmosphere with 5% CO_2, cells were allowed to equilibrate to room temperature and were immediately analyzed on a Luminoskan Ascent Microplate Luminometer (Thermo Fisher Scientific) equipped with an auto-dispenser by addition of coelenterazine substrate to a final concentration of 10 μM in a flash-assay, kinetic format. Integration time was 2000 ms, with two to three measurements performed for each well.

Tumor xenograft animal models in mice

Non-obese diabetic/severe combined immunodeficiency (NOD/SCID) mice (NOD.CB17-*Prkdc*^{scid}, males, 6–8 weeks old) were purchased from and maintained at the Animal Resource Centre (University Health Network, Toronto, ON, Canada).

For the efficacy study, animals were injected subcutaneously on day 0 into their right dorsal flank with 2.5×10^6 PC3 cells, suspended in 100 μl PBS and 100 μl Matrigel Basement Membrane Matrix (354234, BD Biosciences, San Jose, CA, USA) per injection. Animals were treated starting on day 1. Animals were randomized into four treatment groups. Animals in drug-treated groups received a three-times a week (TIW) dose of 3, 0.3, or 0.03 mg/kg of AT-001 (in 20 mM sodium acetate buffer, pH 5.0) subcutaneously, for 8 weeks starting at day 1. Animals in vehicle-treated group received an equivalent volume of the 20 mM sodium acetate, pH 5.0, buffer by s.c. injection. Tumor volume was assessed by caliper measurements weekly and approximated using the formula: length×width×height×π/6. Animals were killed on week 8; tumors were then harvested, photographed, measured with a caliper, weighed, and processed for subsequent analyses.

For the combination treatment study, animals were injected as above with 3×10^6 PC3 cells, and randomized into four treatment groups. Animals in the AT-001- and AT-001/docetaxel-treated groups received a TIW dose of 0.3 mg/kg AT-001 (in 20 mM sodium acetate buffer, pH 5.0) subcutaneously, for 5 weeks starting at week 2.5 (middle of week 3). Animals in the docetaxel- and AT-001/docetaxel-treated groups received four weekly (Q7D×4) i.v. injections of 10 mg/ml docetaxel. Animals in vehicle-treated group received an equivalent volume of the 20 mM sodium acetate, pH 5.0, subcutaneously. Animals were killed on week 8 and processed as above.

Immunohistochemistry

A portion of each harvested tumor was fixed in neutral buffered formalin, paraffin embedded, sectioned, and several sections from each tumor were stained with a 1:1000 dilution of the rabbit anti-mouse CD31 (PECAM-1) antibody (SC-1506-R, Santa Cruz Biotechnology, Inc.) to

http://erc.endocrinology-journals.org
DOI: 10.1530/ERC-14-0088

Published by Bioscientifica Ltd.

visualize vascular endothelium. Slides were stained on the Ventana Benchmark XT stainer (Ventana Medical Systems, Tucson, AZ, USA) using the iVIEW DAB detection system (Ventana Medical Systems). Intratumoral and extratumoral average microvessel areas (MVAs) were determined for each tumor by identifying four intratumoral and four extratumoral regions of increased density of vascular endothelial cells, termed 'hot spots', from two to three serial tumor cross sections, and measuring, under a 200× magnification, the cross-sectional areas of all microvessels in each region. The areas of three largest microvessels were averaged for each region analyzed, and the average across analyzed regions yielded the respective MVAs. Intratumoral and extratumoral microvessel densities (MVDs) were determined by counting the number of stained microvessels in each 'hot spot' analyzed (normalized to unit area). Total MVAs and MVDs for each treatment group were calculated by averaging the MVAs and MVDs, respectively, from each tumor within the group. All sections were examined using a Leica DM1000 phase-contrast microscope (Leica Microsystems, Concord, ON, Canada), and images were captured at 200× magnification using a Leica EC3 camera and analyzed using the Leica Application Suite Software (ver. 4.0.0).

Western blotting

A portion of each tumor was flash frozen, and a small portion was resected and lysed by sonication in RIPA lysis buffer (Thermo Fisher Scientific) containing a protease inhibitor cocktail (Complete Ultra Mini Tables, EDTA-free, Roche) and 1 mM phenylmethanesulfonyl fluoride (Sigma–Aldrich). For each treatment group, an equivalent amount of protein lysate was pooled by total protein content from each tumor for a total of 150 μg/group. Pooled lysates were resolved by 7% SDS–PAGE in duplicate and blotted onto a PVDF membrane (Immobilon-P, EMD Millipore, Billerica, MA, USA). Membranes were blocked in 5% non-fat dried milk (NFDM) in 0.05% Tween 20–PBS (T–PBS) at 4°C overnight. Membranes were probed in 1% NFDM in T–PBS for either hypoxia-inducible factor 1 alpha (HIF1α) with 10 μg/ml monoclonal mouse anti-HIF1α antibody (clone #241809, R&D Systems, Minneapolis, MN, USA) or a 1:5000 dilution of the monoclonal mouse anti-α-tubulin (Sigma–Aldrich) as a loading control for 2 h at room temperature. Subsequently, membranes were probed with a 1:3000 dilution of the secondary goat anti-mouse IgG–HRP conjugate antibody (Bio-Rad) in 1% NFDM in T–PBS for 1 h at room temperature. Membranes were developed using the SuperSignal West Pico Substrate Kit (Pierce, Thermo Fisher Scientific) and exposed on film. Densitometry was performed on a film with moderate exposure using the Image Lab Software (ver. 3.0, Bio-Rad).

RNA disruption assay

A portion of each harvested tumor, ~10 mg in size, was preserved in the RNAlater fixative (Life Technologies). Following permeation and stabilization in RNAlater overnight at room temperature, samples were frozen for storage until analysis. Total RNA was isolated using the Qiagen miRNeasy Kit (Qiagen) from individual samples and analyzed using an Agilent Bioanalyzer 2100 (Agilent, Pleasanton, CA, USA). Data from the resulting RNA electropherograms were analyzed using proprietary algorithms and an RNA disruption index (RDI) value was established for each RNA isolate.

Ethics statement

All animal experimental procedures followed a protocol approved by the Animal Care Committee of the University Health Network (Toronto, ON, Canada). Animals were maintained at the Animal Resource Centre (University Health Network) colony at the Canadian Blood Services Building.

Statistical analysis

Statistical significance between groups was evaluated by Student's *t*-test or one-way ANOVA analyses, with Dunnett's *post hoc* comparison test, as applicable, using GraphPad Prism (ver. 5.0, GraphPad Software, San Diego, CA, USA). The log-rank (Mantel–Cox) test was used for the comparison of survival curves.

Results

Synthesis and characterization of AT-001's binding and antagonist properties

AT-001 is a synthetic analog of human H2 relaxin with Arg13 and Arg17 in the RBD within the B-chain substituted with lysine residues (Silvertown *et al.* 2007, Hossain *et al.* 2010). To confirm that the chemically synthesized AT-001 retained its binding ability to the primary relaxin receptor, RXFP1, H2 relaxin was labeled with ^{125}I using the Pierce iodination reagent (Millar & Smith 1983), which radioiodinates the phenol aromatic ring of Tyr residues (Tyr3 on the A-chain). In an *in vitro* cell-based assay utilizing the 293T.RXFP1 cell line (engineered to overexpress RXFP1), we

http://erc.endocrinology-journals.org
DOI: 10.1530/ERC-14-0088

Published by Bioscientifica Ltd.

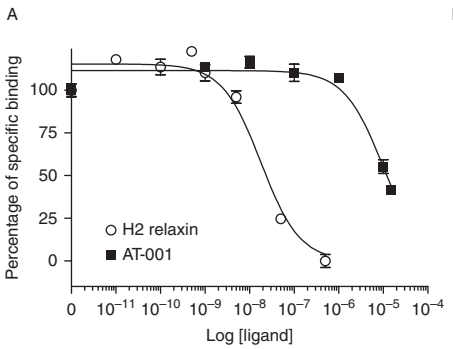

B

Ligand	pK_d/pK_i	K_d/K_i
H2 relaxin	7.769	17.0 nM
AT-001	5.034	9.242 μM

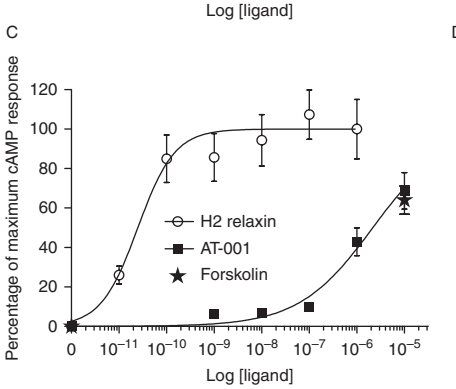

D

Ligand	pEC_{50}	EC_{50}
H2 relaxin	10.60	24.9 pM
AT-001	5.664	2.17 μM

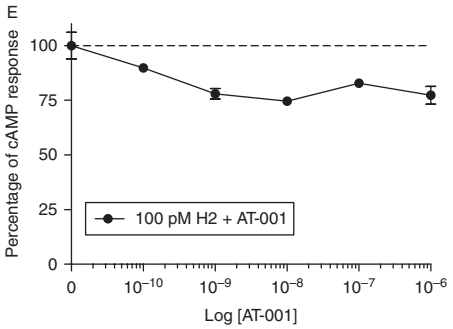

Figure 1

AT-001 is a relaxin receptor antagonist. (A) Binding of H2 relaxin and AT-001 to RXFP1 evaluated by a radioligand-binding assay with ^{125}I-labeled H2 relaxin on 293T.RXFP1 cells. Specific binding of 1 nM ^{125}I-labeled H2 relaxin was measured in the presence of increasing concentrations of 'cold' H2 relaxin (open circles) or AT-001 (closed squares). All assays were performed in triplicate. Data represent mean ± S.E.M. Data were fitted using a one-site competitive binding model (R^2 = 0.96 and 0.94, for H2 relaxin and AT-001 respectively). (B) Summary of equilibrium dissociation (K_d) and inhibition (K_i) constants derived for H2 relaxin and AT-001 respectively. (C) Ability of H2 relaxin and AT-001 to induce cAMP signaling measured on HEK293.RXFP1.mGL.2 cells by a luciferase-based reporter assay. H2 relaxin (open circles) and AT-001 (closed squares) induce expression of luciferase under the control of the cAMP response element (CRE) in a dose-dependent manner. All assays were performed at least in duplicate. Data represent mean ± S.E.M. Data were fitted using a sigmoidal, variable Hill slope model (R^2 = 0.90 and 0.95, for H2 relaxin and AT-001 respectively). (D) Summary of EC_{50} parameters derived for cAMP stimulation by H2 relaxin and AT-001. (E) Induction of cAMP signaling assessed in a competitive luciferase assay format on HEK293.RXFP1.mGL.2 cells by measuring the induction of luciferase expression by 100 pM H2 relaxin in the presence of increasing concentrations of AT-001 (closed circles). Dotted line denotes luciferase activity in the absence of inhibition by AT-001. Data represent mean ± S.E.M. All assays were performed in triplicate.

showed that H2 relaxin binds to RXFP1 with a K_d of 17.0 nM in a homologous competitive RBA format (Fig. 1A and B). Similarly, AT-001 was shown to retain the binding capacity for RXFP1 in a competitive RBA, inhibiting binding of ^{125}I-labeled H2 relaxin with a K_i of 9.2 μM (Fig. 1A and B).

To confirm that AT-001 exhibits impaired signaling properties, we evaluated its ability to stimulate cAMP signaling, the standard measure of activation of the relaxin pathway. H2 relaxin was able to stimulate cAMP signaling in a dose-dependent manner with an EC_{50} of 24.9 pM (Fig. 1C and D). In contrast to H2 relaxin, AT-001 exhibited limited activity up to micromolar concentrations, with an EC_{50} of 2.17 μM in the same assay (Fig. 1C and D), confirming previous findings about this modification of

http://erc.endocrinology-journals.org
DOI: 10.1530/ERC-14-0088

Published by Bioscientifica Ltd.

the RBD (Silvertown *et al.* 2007, Hossain *et al.* 2010). Partial agonist properties of AT-001 can result in a basal level of signaling that would be dependent on the relaxin receptor density and sensitivity of the stimulated cells, consistent with the *in vitro* observation on the HEK293.RXFP1 cells (Fig. 1C), which are engineered to express supra-physiological levels of RXFP1. The ability of AT-001 to act as a competitive antagonist to human H2 relaxin on these cells was evaluated by measuring cAMP stimulation by 100 pM H2 relaxin (~80% of maximal cAMP response) in the presence of increasing concentrations of AT-001 (Fig. 1E). AT-001 suppressed signaling induced with 100 pM H2 relaxin by ~25% at AT-001 concentrations >1 nM (Fig. 1E). Taken together, these results confirmed *in vitro* that AT-001 binds to RXFP1 but exhibits significant functional impairment in signaling capacity.

AT-001 suppresses growth of aggressive, androgen-independent PC3 prostate carcinoma-derived xenografts *in vivo*

We have previously shown that a recombinant form of AT-001, expressed in PC3 tumor xenografts, suppressed tumor growth (Silvertown *et al.* 2007). PC3 cells express RXFP1 (Silvertown *et al.* 2006*b*, 2007), secrete H2 relaxin *in vivo* (Silvertown *et al.* 2006*b*), and express H2 relaxin transcripts (Gunnersen *et al.* 1995, Feng *et al.* 2007). To support AT-001 as a drug candidate for tumor growth suppression to be delivered subcutaneously, a similar tumor xenograft model was employed. NOD/SCID mice were inoculated with the androgen-independent PC3 human prostate cancer cell line in their right flank and treated with either vehicle control or increasing doses of AT-001 delivered by s.c. injection three times a week. Pharmacokinetic studies of i.v. vs s.c. H2 relaxin have shown that

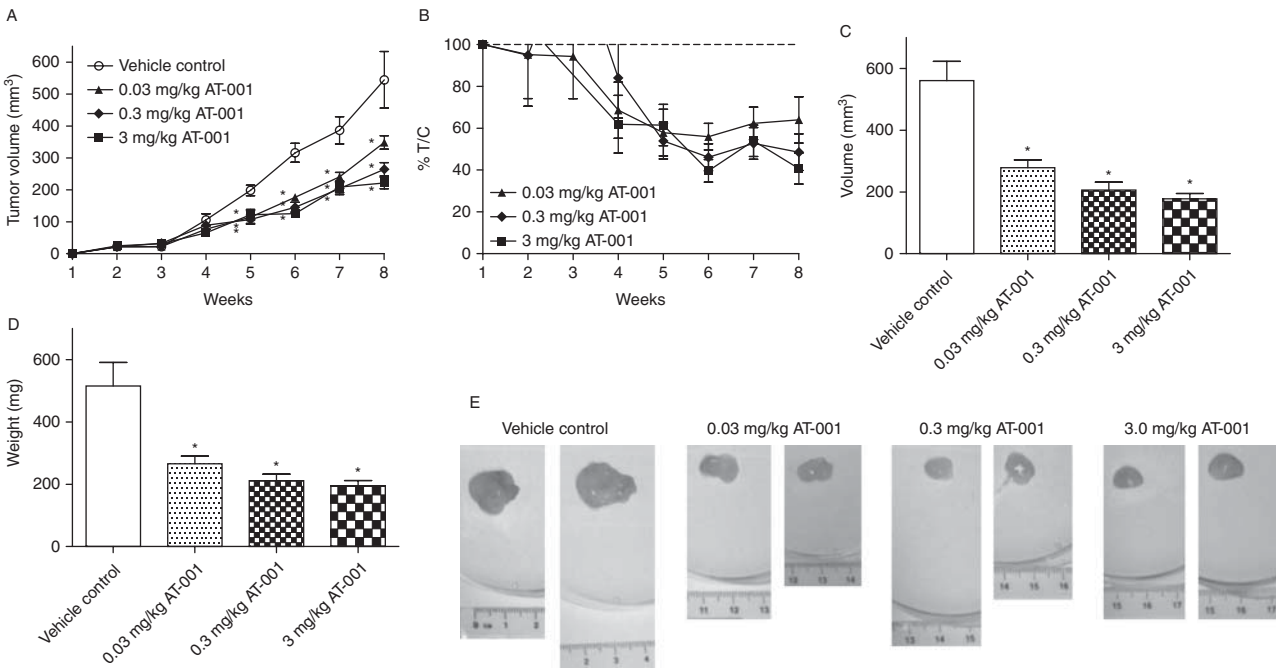

Figure 2

AT-001 suppresses the growth of androgen-independent PC3 prostate carcinoma xenografts in a dose-dependent manner. (A) Xenografts were established by implantation of 2.5×10^6 PC3 cells into the right dorsal flank of male NOD/SCID mice ($n=10$). Animals were treated TIW for 8 weeks with either s.c. vehicle (open circles) or AT-001 at doses of 0.03 mg/kg (closed triangles), 0.3 mg/kg (closed diamonds), or 3 mg/kg (closed squares). Tumor dimensions (length, width, and depth) were measured weekly with a caliper to estimate the volume. Data represent mean±s.e.m. Statistical significance is indicated (*$P<0.05$, treatment vs vehicle control). (B) Percentage of treatment over control (% T/C) for each treatment group, calculated as the mean relative tumor volume (RTV) of the treatment group over the mean RTV of the control group multiplied by 100%. Data represent mean±s.e.m. (C) Average endpoint tumor volume for each treatment group assessed by measuring the dimensions of the harvested tumors with a caliper. Data represent mean±s.e.m. Statistical significance is indicated (*$P<0.01$, treatment vs vehicle control). (D) Average endpoint tumor weight for each treatment group assessed by weighing each harvested tumor. Data represent mean±s.e.m. Statistical significance is indicated (*$P<0.01$, treatment vs vehicle control). (E) Images (photographed against a centimeter ruler) of representative harvested tumors at study endpoint from each treatment group.

http://erc.endocrinology-journals.org
DOI: 10.1530/ERC-14-0088

Published by Bioscientifica Ltd.

s.c. administration results in a sustained release with a significantly longer serum half-life (Moore & Wroblewski 1992). At all doses evaluated, AT-001 was able to significantly suppress tumor growth compared with vehicle-treated control by up to 60% (Fig. 2A), with a % T/C of up to 40% (Fig. 2B) and a tumor growth delay of ~2 weeks. The lowest dosing of AT-001 examined, 0.03 mg/kg TIW, was sufficient to achieve a close-to-maximum tumor growth suppression in this model (Fig. 2A and B). *In vivo* caliper-based tumor volume measurements were consistent with *ex vivo* measurements of tumor volumes (Fig. 2C) and weights (Fig. 2D) on harvested tumors. All tumors were photographed, and representative tumors are shown (Fig. 2E), demonstrating the significant reduction in tumor volumes observed in the AT-001-treated groups compared with vehicle-treated controls. No toxicity or adverse events were observed due to AT-001 injections.

Anti-angiogenic properties of AT-001 contribute to impairment of tumor growth

We have previously shown that antagonizing the relaxin signaling pathway in prostate tumor xenografts exerts an anti-angiogenic effect as one of the contributing mechanisms to impairing tumor growth (Silvertown *et al*. 2007). To examine the impact of AT-001 on tumoral microvasculature, AT-001- and vehicle-treated tumors were harvested and analyzed by immunohistochemistry to evaluate the intratumoral and extratumoral (immediately surrounding the tumor boundary) microvasculature by staining for mouse CD31 (PECAM-1), a marker for endothelial cells. Both average extratumoral and intratumoral mean MVAs (Fig. 3A and B respectively) of the AT-001-treated tumors were significantly reduced compared with tumors from the vehicle-treated group. However, no significant reduction was detected in MVD

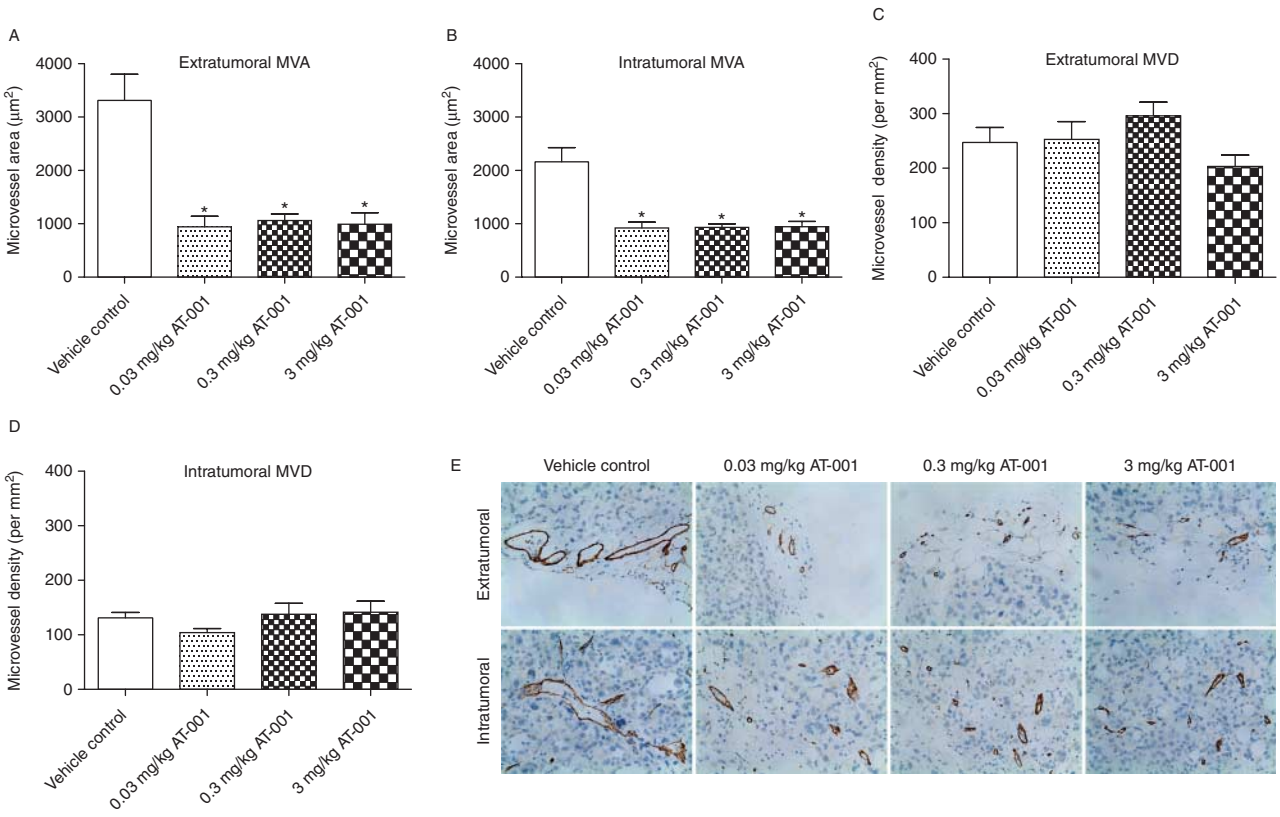

Figure 3

AT-001 exerts an anti-angiogenic effect on PC3 tumor xenografts. (A and B) Mean microvessel area (MVA) (A) in the periphery of the tumors (extratumoral) and (B) within the tumors (intratumoral). Data represent mean±S.E.M. (n=9–10). Statistical significance is indicated (*P<0.0001, treatment vs vehicle control). (C and D) Mean microvessel density (MVD) (C) in the periphery of the tumors (extratumoral) and (D) within the tumors (intratumoral). Data represent mean±S.E.M. (n=9–10). (E) Immunohistochemistry staining for CD31 of representative tumor cross sections from AT-001- and vehicle-treated groups (200× magnification).

http://erc.endocrinology-journals.org
DOI: 10.1530/ERC-14-0088

Published by Bioscientifica Ltd.

(Fig. 3C and D respectively). Figure 3E depicts representative immunohistochemistry sections from AT-001-treated and vehicle-treated tumors, highlighting the observed reduction in MVAs in AT-001-treated tumors. These findings support the anti-angiogenic activity of AT-001 as one of the mechanisms impairing tumor growth.

AT-001 synergizes with chemotherapeutic agents acting on the hypoxia-induced response

The hallmark of anti-angiogenic therapy is the creation of a hypoxic environment in the tumor, which triggers the hypoxia-induced response (Rapisarda & Melillo 2009). This leads to an adaptation to hypoxic growth by a number of different mechanisms, including compensatory angiogenesis (Gu *et al*. 2006), autophagy (Hu *et al*. 2012), metabolic changes (Keunen *et al*. 2011), and increased invasiveness (Pennacchietti *et al*. 2003). Transient effectiveness and resistance to anti-angiogenic therapy have been documented in numerous models, including in PC3 cells (Voss *et al*. 2010, Weisshardt *et al*. 2012). Therapeutics with an anti-angiogenic mechanism of action can greatly benefit from agents that specifically target the hypoxia-induced response. The transcription factor subunit HIF1α (HIF1A) is a master regulator of the hypoxia-induced response (Semenza 2002), is upregulated by androgen (Mabjeesh *et al*. 2003), and plays an important role in the progression and aggressiveness of androgen-insensitive prostate cancer (Jeong *et al*. 2012). Several agents achieve significant inhibition of HIF1α and the hypoxia-induced response, including a variety of microtubule-targeted drugs such as docetaxel (Escuin *et al*. 2005, Forde *et al*. 2012). This study determined that the combined treatment of androgen-insensitive xenografts with AT-001 and docetaxel results in synergistic efficacy. NOD/SCID mice were treated with vehicle-treated control, AT-001, docetaxel, or both AT-001 and docetaxel at 2.5 weeks after inoculation with PC3 cells. Guided by the observed efficacy of AT-001 in suppressing tumor growth (Fig. 2), a 0.3 mg/kg dose level was employed. AT-001 and docetaxel treatments alone significantly suppressed tumor growth by ∼40 and 95% respectively (Fig. 4A and C). The combination of AT-001 and docetaxel treatment (>98% suppression of tumor growth) resulted in a significantly more impaired tumor growth when compared with the docetaxel only-treated tumors (Fig. 4B), suggesting that AT-001 and docetaxel acted in concert. Endpoint *ex vivo* tumor volume measurements on harvested tumors confirmed significantly smaller tumors in the combination treatment group (27.03 ± 9.73 mm^3) compared with the docetaxel-treated group (48.31 ± 4.63 mm^3).

To determine whether AT-001 and docetaxel synergized in impairing prostate cancer xenografts in the PC3 model, we needed to delineate the relative contribution of the different mechanisms of action of each treatment. Expression of HIF1α in tumor lysates from each group was examined. HIF1α is rapidly degraded under normoxic conditions, but is upregulated under hypoxic conditions (Cheng *et al*. 2007). Vehicle-treated PC3 tumors had detectable HIF1α expression (Fig. 5A), consistent with a hypoxic tumor environment that would trigger the hypoxia-induced response in these cells, which are also

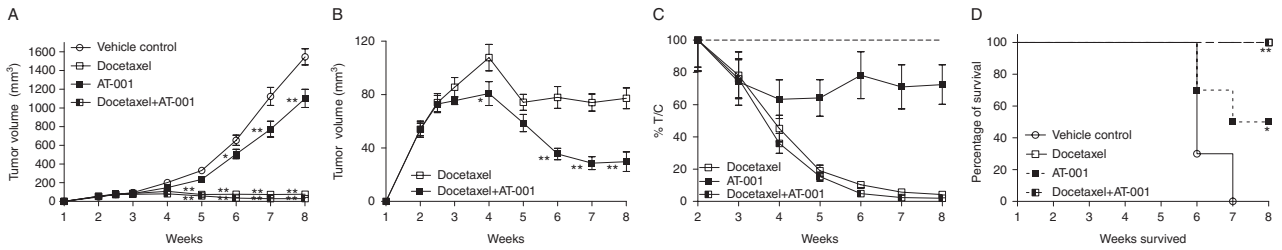

Figure 4

AT-001 enhances the efficacy of docetaxel chemotherapy in PC3 tumor xenografts. (A) Xenografts were established by implantation of 3×10^6 PC3 cells into the right dorsal flank of male NOD/SCID mice ($n = 10$–11). Starting in the middle of weeks 3, animals were treated TIW for 5 weeks with vehicle (open circles), or 0.3 mg/kg AT-001 subcutaneously with (semi-closed squares) or without (closed squares) docetaxel. Animals in docetaxel only (open squares) and docetaxel + AT-001 (semi-closed squares) treatment groups were treated intravenously with four-times weekly (Q7D) injections of 10 mg/kg docetaxel. Tumor dimensions (length, width, and depth) were measured weekly with a caliper to estimate the volume. Data represent mean ± S.E.M. Statistical significance is indicated (*P<0.05 or **P<0.001, treatment vs vehicle control). (B) Tumor volumes in the docetaxel-treated groups, with (closed squares) or without (open squares) AT-001 treatment. Data represent mean ± S.E.M. Statistical significance is indicated (*P<0.05 or **P<0.001, treatment vs vehicle control). (C) Percentage of treatment over control (% T/C) for each treatment group, calculated as the mean relative tumor volume (RTV) of the treatment group over the mean RTV of the control group multiplied by 100%. Data represent mean ± S.E.M. (D) Kaplan–Meier survival analysis of mice bearing tumors in each treatment group (mice bearing tumors of >1000 mm^3 in volume were considered as moribund). Statistical significance is indicated (*P<0.05 or **P<0.001, treatment vs vehicle control).

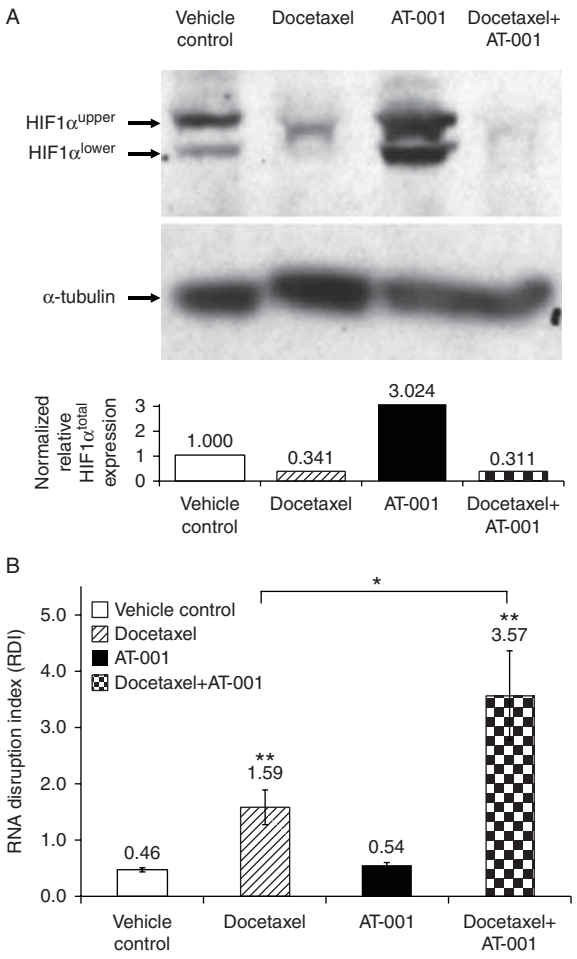

Figure 5
AT-001 synergizes with docetaxel treatment. (A) Evaluation of the hypoxia-induced response by western blot analysis of the expression of HIF1α. Effect of treatment with docetaxel (diagonal shading), AT-001 (black bar), or a combination of docetaxel and AT-001 (checkerboard shading) on the expression of HIF1α in pooled lysates from harvested tumors compared with pooled lysates from vehicle-treated controls (white bar) ($n=10$–11 per group). HIF1α^{total} (combined expression of HIF1α^{upper} band and HIF1α^{lower} band expression) was quantified by densitometry along with α-tubulin as a loading control. Relative expression of HIF1α is indicated, normalized to α-tubulin. Representative data from three independent repeats are shown. (B) RNA disruption index (RDI) in groups treated with vehicle (white bar), docetaxel (diagonal shading), AT-001 (black bar), or a combination of docetaxel and AT-001 (checkerboard shading), as assessed by the RNA disruption assay (RDA) in RNA preparation from harvested tumors ($n=10$–11). Data represent mean±s.e.m. Statistical significance is indicated (*$P<0.05$, docetaxel vs docetaxel+AT-001 and **$P<0.01$, treatment vs vehicle control).

known to express high HIF1α even under normoxic conditions (Zhong *et al.* 1998). AT-001-treated tumors exhibited a threefold increase in HIF1α expression over vehicle-treated controls (Fig. 5A), suggesting that the anti-angiogenic activity of AT-001 has triggered an increased hypoxia-induced response. Docetaxel treatment significantly downregulated the expression of HIF1α in treated tumors (Fig. 5A), reducing the expression of HIF1α by >65% compared with the vehicle-treated control group. Moreover, docetaxel acted synergistically with AT-001 by decreasing HIF1α expression in the combination treatment group by ~90% compared with the AT-001-treated group (Fig. 5A). Docetaxel likely increased the sensitivity of treated tumors to the anti-angiogenic effects of AT-001, while concomitantly downregulating the compensatory angiogenesis promoted by HIF1α.

To delineate the contribution of anti-angiogenic and other effects mediated by AT-001 from the cytotoxic activity of docetaxel, we evaluated the disruption of rRNA in the harvested tumors by the RNA disruption assay. RNA disruption is associated with tumor response to chemotherapy, including such cytotoxic agents as docetaxel (Parissenti *et al.* 2010). Consistent with this, we observed a significant increase (greater than threefold) in the RDI, a measure of rRNA disruption, in the docetaxel-treated tumors (Fig. 5B). No increase in RDI was induced by AT-001, as evidenced from tumors treated with AT-001 alone (Fig. 5B), indicating that RDI is only sensitive to the effects of docetaxel. The RDI value increased by more than sevenfold in the combination treatment group of AT-001 and docetaxel (Fig. 5B) compared with the vehicle-treated control groups or AT-001-treated groups. AT-001 treatment clearly potentiated the effects of docetaxel, as reflected in the results of this assay. Taken together, this indicates that AT-001 synergized with docetaxel to result in increased RNA disruption in tumors concomitantly treated with both agents. These data parallel the finding that a greater decrease in tumor mass was observed in the combination treatment group compared with either treatment alone (Fig. 4A and B).

Discussion

In the previous work, we and others have demonstrated that suppressing the relaxin signaling pathway in androgen-sensitive (LNCaP) and androgen-insensitive, AR-negative (PC3) prostate cancer xenografts impairs their growth *in vivo* (Silvertown *et al.* 2007, Feng *et al.* 2010). In this study, we functionally confirmed the *in vivo* efficacy of a new anti-hormonal drug candidate, AT-001, targeting the relaxin hormone signaling pathway in a prostate cancer model. AT-001, an antagonist of the human H2 relaxin receptor, exhibits significant potency in impairing tumor growth in an aggressive model of androgen-insensitive prostate cancer. PC3 tumor xenografts are devoid of AR expression (van Bokhoven *et al.* 2003) and represent a model of an advanced, androgen-

http://erc.endocrinology-journals.org
DOI: 10.1530/ERC-14-0088

Published by Bioscientifica Ltd.

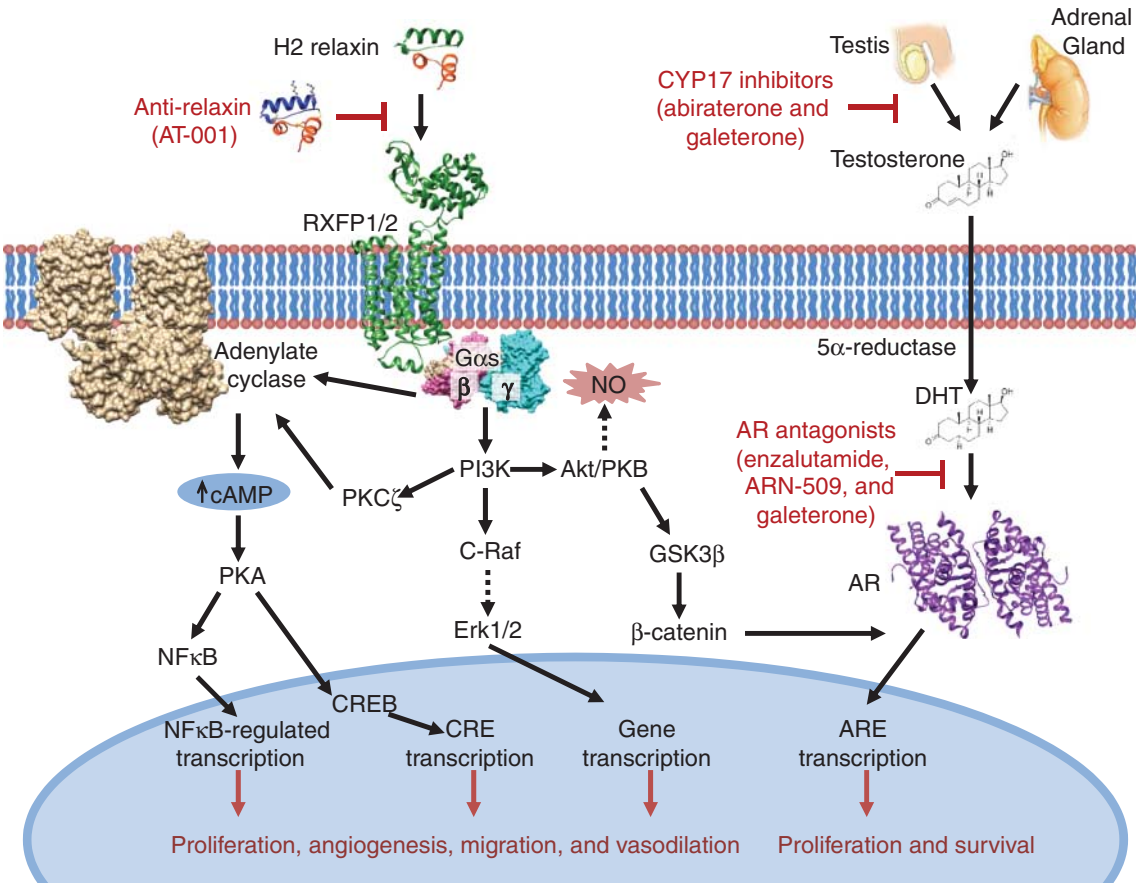

Figure 6

An anti-relaxin therapy, such as AT-001, could exhibit multiple mechanisms of action. Anti-relaxin therapy targets multiple mechanisms of action in prostate cancer. Signaling pathways affected by anti-relaxin and anti-androgen therapies in prostate cancer (red) are depicted along with the key signaling mediators and impacted cellular functions. Akt/PKB, protein kinase B; ARE, androgen response element; C-Raf, rapidly accelerated fibrosarcoma kinase; CRE, cAMP response element; CREB, CRE-binding protein; DHT, dihydrotestosterone; Erk1/2, extracellular signal-regulated kinases 1/2; GSK3β, glycogen synthase kinase 3 beta; NFκB, nuclear factor kappa-light-chain-enhancer of activated B cells; PI3K, phosphatidylinositide 3-kinase; PKA, protein kinase A; PKCζ, protein kinase C zeta.

independent form of human prostate cancer for which few treatment options are currently available. Owing to the lack of AR expression in PC3 cells, other anti-hormonal drugs targeting the AR pathway (anti-androgen class), such as CYP17A1 inhibitors (e.g. abiraterone acetate and galeterone) and AR antagonists (e.g. enzalutamide and ARN-509), have or are expected to have demonstrated limited to no efficacy in androgen-independent cells or tumor xenografts (Mostaghel *et al.* 2011, Zhang *et al.* 2011, Clegg *et al.* 2012). The efficacy demonstrated by AT-001 in the PC3 model (tumor reduction by 60%), which is highly resistant to hypoxia-induced apoptosis (Coffey *et al.* 2005), surpasses the efficacy observed in this model with other types of anti-angiogenic agents, such as bevacizumab (Newman *et al.* 2007, Xu *et al.* 2012), likely owing to the fact that AT-001 is antagonizing multiple pathways downstream of relaxin receptor signaling (Fig. 6) (Silvertown *et al.* 2007). Treatment with increasing doses of AT-001 appeared to reach a plateau in the current prostate cancer model, suggesting that, even at the lower dose levels in this study, AT-001 may have completely antagonized the contribution of the relaxin signaling pathway to promoting the growth of PC3 tumors. AT-001 synergized with docetaxel chemotherapy to curb PC3 tumor growth via a mechanism that involved the down-regulation of hypoxia-induced response. When combined with AT-001, docetaxel dosing regimens could be lowered, reducing the risk of chemotherapy-associated toxicity in prostate cancer patients. It is conceivable that AT-001 could be successfully combined with other chemotherapeutic agents that downregulate HIF1α to synergistically curb the growth of aggressive tumors.

http://erc.endocrinology-journals.org
DOI: 10.1530/ERC-14-0088

Published by Bioscientifica Ltd.

Other strategies targeting RXFP1 have also demonstrated suppression of tumor growth (Feng *et al.* 2010); however, targeting cells expressing RXFP1 by conventional approaches, such as mAb therapeutics, is not an optimal therapeutic strategy given the broad pattern of RXFP1 expression in a multitude of normal tissues beyond the prostate (Hsu *et al.* 2000, Ivell *et al.* 2003). Compared with other biological therapeutics, such as mAbs, AT-001 is sufficiently small to result in good tumor penetration. Development of small molecule-based RXFP1 antagonists would not be trivial given the lack of X-ray crystal structure and appropriate bioassays, and the general difficulty associated with developing small molecules that modulate GPCRs (Fujioka & Omori 2012). However, some progress has recently been made in developing a small-molecule agonist of RXFP1 (Xiao *et al.* 2013).

Collectively, the presented data support the clinical development of AT-001 as a new candidate class of anti-hormonal drugs, either as a monotherapy or as a combination therapy with other chemotherapeutic agents and/or anti-hormonal drugs, in particular, those targeting the AR pathway (Fig. 6). AT-001 is unique in that it dually targets two hormonal pathways – androgen and relaxin. Unlike second-generation anti-androgens, anti-relaxin therapies could conceivably be continued once prostate cancer transitions to androgen independence and could be given in combination with aggressive chemotherapeutic agents when the cancer becomes metastatic (stage III and beyond). Therefore, relaxin receptor antagonists offer the potential for patients to continue hormone therapy well beyond the point where prostate cancer becomes insensitive or resistant to anti-androgen therapies. With the majority of anti-hormonal drugs for prostate cancer targeting the AR pathway, an anti-relaxin therapy represents a promising new approach for the clinic.

Supplementary data
This is linked to the online version of the paper at http://dx.doi.org/10.1530/ERC-14-0088.

Declaration of interest
A Neschadim and J D Silvertown are employees of Armour Therapeutics, Inc. (Toronto, ON, Canada). L B Pritzker and K P H Pritzker are employees of Rna Diagnostics, Inc. (Toronto, ON, Canada). D R Branch, A J S Summerlee, and J Trachtenberg have no conflicts of interest to declare.

Funding
This work was supported by Armour Therapeutics, Inc. (Toronto, ON, Canada).

Author contribution statement
A Neschadim and J D Silvertown contributed to the conception and design of the studies, method development, analysis and interpretation of data, and the writing, review, and revision of the article. A Neschadim, J D Silvertown, L B Pritzker, and K P H Pritzker contributed to different aspects of experimental implementation. D R Branch, A J S Summerlee, and J Trachtenberg contributed to the writing, review, and revision of the article.

Acknowledgements
The authors would like to thank Nicholas Tchernov for his help with the acquisition of immunohistochemistry slides.

References

van Bokhoven A, Varella-Garcia M, Korch C, Johannes WU, Smith EE, Miller HL, Nordeen SK, Miller GJ & Lucia MS 2003 Molecular characterization of human prostate carcinoma cell lines. *Prostate* **57** 205–225. (doi:10.1002/pros.10290)

Carles J, Castellano D, Climent MA, Maroto P, Medina R & Alcaraz A 2012 Castration-resistant metastatic prostate cancer: current status and treatment possibilities. *Clinical & Translational Oncology* **14** 169–176. (doi:10.1007/s12094-012-0780-8)

Cheng J, Kang X, Zhang S & Yeh ET 2007 SUMO-specific, protease 1 is essential for stabilization of HIF1α during hypoxia. *Cell* **131** 584–595. (doi:10.1016/j.cell.2007.08.045)

Clegg NJ, Wongvipat J, Joseph JD, Tran C, Ouk S, Dilhas A, Chen Y, Grillot K, Bischoff ED, Cai L *et al.* 2012 ARN-509: a novel antiandrogen for prostate cancer treatment. *Cancer Research* **72** 1494–1503. (doi:10.1158/0008-5472.CAN-11-3948)

Coffey RN, Morrissey C, Taylor CT, Fitzpatrick JM & Watson RW 2005 Resistance to caspase-dependent, hypoxia-induced apoptosis is not hypoxia-inducible factor-1 alpha mediated in prostate carcinoma cells. *Cancer* **103** 1363–1374. (doi:10.1002/cncr.20918)

Escuin D, Kline ER & Giannakakou P 2005 Both microtubule-stabilizing and microtubule-destabilizing drugs inhibit hypoxia-inducible factor-1alpha accumulation and activity by disrupting microtubule function. *Cancer Research* **65** 9021–9028. (doi:10.1158/0008-5472.CAN-04-4095)

Feng S, Agoulnik IU, Bogatcheva NV, Kamat AA, Kwabi-Addo B, Li R, Ayala G, Ittmann MM & Agoulnik AI 2007 Relaxin promotes prostate cancer progression. *Clinical Cancer Research* **13** 1695–1702. (doi:10.1158/1078-0432.CCR-06-2492)

Feng S, Agoulnik IU, Truong A, Li Z, Creighton CJ, Kaftanovskaya EM, Pereira R, Han HD, Lopez-Berestein G, Klonisch T *et al.* 2010 Suppression of relaxin receptor RXFP1 decreases prostate cancer growth and metastasis. *Endocrine-Related Cancer* **17** 1021–1033. (doi:10.1677/ERC-10-0073)

Forde JC, Perry AS, Brennan K, Martin LM, Lawler MP, Lynch TH, Hollywood D & Marignol L 2012 Docetaxel maintains its cytotoxic activity under hypoxic conditions in prostate cancer cells. *Urologic Oncology* **30** 912–919. (doi:10.1016/j.urolonc.2010.08.015)

Fujioka M & Omori N 2012 Subtleties in GPCR drug discovery: a medicinal chemistry perspective. *Drug Discovery Today* **17** 1133–1138. (doi:10.1016/j.drudis.2012.06.010)

Garmey EG, Sartor O, Halabi S & Vogelzang NJ 2008 Second-line chemotherapy for advanced hormone-refractory prostate cancer. *Clinical Advances in Hematology & Oncology* **6** 118–122 (127–132).

Gu J, Yamamoto H, Ogawa M, Ngan CY, Danno K, Hemmi H, Kyo N, Takemasa I, Ikeda M, Sekimoto M *et al.* 2006 Hypoxia-induced up-regulation of angiopoietin-2 in colorectal cancer. *Oncology Reports* **15** 779–783. (doi:10.3892/or.15.4.779)

Published by Bioscientifica Ltd.

Gulley J, Figg WD & Dahut WL 2003 Treatment options for androgen-independent prostate cancer. *Clinical Advances in Hematology & Oncology* **1** 49–57.

Gunnersen JM, Roche PJ, Tregear GW & Crawford RJ 1995 Characterization of human relaxin gene regulation in the relaxin-expressing human prostate adenocarcinoma cell line LNCaP.FGC. *Journal of Molecular Endocrinology* **15** 153–166. (doi:10.1677/jme.0.0150153)

Heinlein CA & Chang C 2004 Androgen receptor in prostate cancer. *Endocrine Reviews* **25** 276–308. (doi:10.1210/er.2002-0032)

Hombach-Klonisch S, Bialek J, Trojanowicz B, Weber E, Holzhausen HJ, Silvertown JD, Summerlee AJ, Dralle H, Hoang-Vu C & Klonisch T 2006 Relaxin enhances the oncogenic potential of human thyroid carcinoma cells. *American Journal of Pathology* **169** 617–632. (doi:10.2353/ajpath.2006.050876)

Hossain MA, Samuel CS, Binder C, Hewitson TD, Tregear GW, Wade JD & Bathgate RA 2010 The chemically synthesized human relaxin-2 analog, B-R13/17K H2, is an RXFP1 antagonist. *Amino Acids* **39** 409–416. (doi:10.1007/s00726-009-0454-1)

Hsu SY, Kudo M, Chen T, Nakabayashi K, Bhalla A, van der Spek PJ, van Duin M & Hsueh AJ 2000 The three subfamilies of leucine-rich repeat-containing G protein-coupled receptors (LGR): identification of LGR6 and LGR7 and the signaling mechanism for LGR7. *Molecular Endocrinology* **14** 1257–1271. (doi:10.1210/mend.14.8.0510)

Hu YL, DeLay M, Jahangiri A, Molinaro AM, Rose SD, Carbonell WS & Aghi MK 2012 Hypoxia-induced autophagy promotes tumor cell survival and adaptation to antiangiogenic treatment in glioblastoma. *Cancer Research* **72** 1773–1783. (doi:10.1158/0008-5472.CAN-11-3831)

Ivell R, Balvers M, Pohnke Y, Telgmann R, Bartsch O, Milde-Langosch K, Bamberger AM & Einspanier A 2003 Immunoexpression of the relaxin receptor LGR7 in breast and uterine tissues of humans and primates. *Reproductive Biology and Endocrinology* **1** 114. (doi:10.1186/1477-7827-1-114)

Jeong CW, Yoon CY, Jeong SJ, Hong SK, Byun SS, Kwak C & Lee SE 2012 The role of hypoxia-inducible factor-1alpha and -2alpha in androgen insensitive prostate cancer cells. *Urologic Oncology* **31** 1448–1456. (doi:10.1016/j.urolonc.2012.03.022)

Joseph JD, Lu N, Qian J, Sensintaffar J, Shao G, Brigham D, Moon M, Maneval EC, Chen I, Darimont B *et al*. 2013 A clinically relevant androgen receptor mutation confers resistance to second-generation antiandrogens enzalutamide and ARN-509. *Cancer Discovery* **3** 1020–1029. (doi:10.1158/2159-8290.CD-13-0226)

Kamat AA, Feng S, Agoulnik IU, Kheradmand F, Bogatcheva NV, Coffey D, Sood AK & Agoulnik AI 2006 The role of relaxin in endometrial cancer. *Cancer Biology & Therapy* **5** 71–77. (doi:10.4161/cbt.5.1.2289)

Keunen O, Johansson M, Oudin A, Sanzey M, Rahim SA, Fack F, Thorsen F, Taxt T, Bartos M, Jirik R *et al*. 2011 Anti-VEGF treatment reduces blood supply and increases tumor cell invasion in glioblastoma. *PNAS* **108** 3749–3754. (doi:10.1073/pnas.1014480108)

Korpal M, Korn JM, Gao X, Rakiec DP, Ruddy DA, Doshi S, Yuan J, Kovats SG, Kim S, Cooke VG *et al*. 2013 An F876L mutation in androgen receptor confers genetic and phenotypic resistance to MDV3100 (enzalutamide). *Cancer Discovery* **3** 1030–1043. (doi:10.1158/2159-8290.CD-13-0142)

Liu S, Vinall RL, Tepper C, Shi XB, Xue LR, Ma AH, Wang LY, Fitzgerald LD, Wu Z, Gandour-Edwards R *et al*. 2008 Inappropriate activation of androgen receptor by relaxin via β-catenin pathway. *Oncogene* **27** 499–505. (doi:10.1038/sj.onc.1210671)

Mabjeesh NJ, Willard MT, Frederickson CE, Zhong H & Simons JW 2003 Androgens stimulate hypoxia-inducible factor 1 activation via autocrine loop of tyrosine kinase receptor/phosphatidylinositol 3′-kinase/protein kinase B in prostate cancer cells. *Clinical Cancer Research* **9** 2416–2425.

Millar WT & Smith JF 1983 Protein iodination using iodogen. *International Journal of Applied Radiation and Isotopes* **34** 639–641. (doi:10.1016/0020-708X(83)90068-6)

Moore J & Wroblewski V 1992 Pharmacokinetics and metabolism of protein hormones. In *Protein Pharmacokinetics and Metabolism*, pp 93–126. Eds B Ferraiolo, M Mohler & C Gloff. USA: Springer.

Mostaghel EA, Marck BT, Plymate SR, Vessella RL, Balk S, Matsumoto AM, Nelson PS & Montgomery RB 2011 Resistance to CYP17A1 inhibition with abiraterone in castration-resistant prostate cancer: induction of steroidogenesis and androgen receptor splice variants. *Clinical Cancer Research* **17** 5913–5925. (doi:10.1158/1078-0432.CCR-11-0728)

Newman SP, Foster PA, Ho YT, Day JM, Raobaikady B, Kasprzyk PG, Leese MP, Potter BV, Reed MJ & Purohit A 2007 The therapeutic potential of a series of orally bioavailable anti-angiogenic microtubule disruptors as therapy for hormone-independent prostate and breast cancers. *British Journal of Cancer* **97** 1673–1682. (doi:10.1038/sj.bjc.6604100)

Parissenti AM, Chapman JA, Kahn HJ, Guo B, Han L, O'Brien P, Clemons MP, Jong R, Dent R, Fitzgerald B *et al*. 2010 Association of low tumor RNA integrity with response to chemotherapy in breast cancer patients. *Breast Cancer Research and Treatment* **119** 347–356. (doi:10.1007/s10549-009-0531-x)

Pennacchietti S, Michieli P, Galluzzo M, Mazzone M, Giordano S & Comoglio PM 2003 Hypoxia promotes invasive growth by transcriptional activation of the met protooncogene. *Cancer Cell* **3** 347–361. (doi:10.1016/S1535-6108(03)00085-0)

Rapisarda A & Melillo G 2009 Role of the hypoxic tumor microenvironment in the resistance to anti-angiogenic therapies. *Drug Resistance Updates* **12** 74–80. (doi:10.1016/j.drup.2009.03.002)

Reis LO 2012 Old issues and new perspectives on prostate cancer hormonal therapy: the molecular substratum. *Medical Oncology* **29** 1948–1955. (doi:10.1007/s12032-011-9991-z)

Semenza GL 2002 HIF-1 and tumor progression: pathophysiology and therapeutics. *Trends in Molecular Medicine* **8** S62–S67. (doi:10.1016/S1471-4914(02)02317-1)

Silvertown JD, Summerlee AJ & Klonisch T 2003 Relaxin-like peptides in cancer. *International Journal of Cancer* **107** 513–519. (doi:10.1002/ijc.11424)

Silvertown JD, Walia JS, Summerlee AJ & Medin JA 2006*a* Functional expression of mouse relaxin and mouse relaxin-3 in the lung from an Ebola virus glycoprotein-pseudotyped lentivirus via tracheal delivery. *Endocrinology* **147** 3797–3808. (doi:10.1210/en.2006-0028)

Silvertown JD, Ng J, Sato T, Summerlee AJ & Medin JA 2006*b* H2 relaxin overexpression increases *in vivo* prostate xenograft tumor growth and angiogenesis. *International Journal of Cancer* **118** 62–73. (doi:10.1002/ijc.21288)

Silvertown JD, Symes JC, Neschadim A, Nonaka T, Kao JC, Summerlee AJ & Medin JA 2007 Analog of H2 relaxin exhibits antagonistic properties and impairs prostate tumor growth. *FASEB Journal* **21** 754–765. (doi:10.1096/fj.06-6847com)

Tashima LS, Mazoujian G & Bryant-Greenwood GD 1994 Human relaxins in normal, benign and neoplastic breast tissue. *Journal of Molecular Endocrinology* **12** 351–364. (doi:10.1677/jme.0.0120351)

Thompson VC, Morris TG, Cochrane DR, Cavanagh J, Wafa LA, Hamilton T, Wang S, Fazli L, Gleave ME & Nelson CC 2006 Relaxin becomes upregulated during prostate cancer progression to androgen independence and is negatively regulated by androgens. *Prostate* **66** 1698–1709. (doi:10.1002/pros.20423)

Verhaegent M & Christopoulos TK 2002 Recombinant Gaussia luciferase. Overexpression, purification, and analytical application of a bioluminescent reporter for DNA hybridization. *Analytical Chemistry* **74** 4378–4385. (doi:10.1021/ac025742k)

Vinall RL, Tepper CG, Shi XB, Xue LA, Gandour-Edwards R & de Vere White RW 2006 The R273H p53 mutation can facilitate the androgen-independent growth of LNCaP by a mechanism that involves H2 relaxin and its cognate receptor LGR7. *Oncogene* **25** 2082–2093. (doi:10.1038/sj.onc.1209246)

Voss MJ, Niggemann B, Zanker KS & Entschladen F 2010 Tumour reactions to hypoxia. *Current Molecular Medicine* **10** 381–386. (doi:10.2174/156652410791317020)

http://erc.endocrinology-journals.org
DOI: 10.1530/ERC-14-0088

Published by Bioscientifica Ltd.

Weisshardt P, Trarbach T, Durig J, Paul A, Reis H, Tilki D, Miroschnik I, Ergun S & Klein D 2012 Tumor vessel stabilization and remodeling by anti-angiogenic therapy with bevacizumab. *Histochemistry and Cell Biology* **137** 391–401. (doi:10.1007/s00418-011-0898-8)

Xiao J, Huang Z, Chen CZ, Agoulnik IU, Southall N, Hu X, Jones RE, Ferrer M, Zheng W, Agoulnik AI *et al.* 2013 Identification and optimization of small-molecule agonists of the human relaxin hormone receptor RXFP1. *Nature Communications* **4** 1953. (doi:10.1038/ncomms2953)

Xu Y, Chang E, Liu H, Jiang H, Gambhir SS & Cheng Z 2012 Proof-of-concept study of monitoring cancer drug therapy with Cerenkov luminescence imaging. *Journal of Nuclear Medicine* **53** 312–317. (doi:10.2967/jnumed.111.094623)

Yuan X, Cai C, Chen S, Yu Z & Balk SP 2013 Androgen receptor functions in castration-resistant prostate cancer and mechanisms of resistance to new agents targeting the androgen axis. *Oncogene* [in press]. (doi:10.1038/onc.2013.235)

Zhang Y, Castaneda S, Dumble M, Wang M, Mileski M, Qu Z, Kim S, Shi V, Kraft P, Gao Y *et al.* 2011 Reduced expression of the androgen receptor by third generation of antisense shows antitumor activity in models of prostate cancer. *Molecular Cancer Therapeutics* **10** 2309–2319. (doi:10.1158/1535-7163.MCT-11-0329)

Zhong H, Agani F, Baccala AA, Laughner E, Rioseco-Camacho N, Isaacs WB, Simons JW & Semenza GL 1998 Increased expression of hypoxia inducible factor-1alpha in rat and human prostate cancer. *Cancer Research* **58** 5280–5284.

Received in final form 25 March 2014
Accepted 8 April 2014

http://erc.endocrinology-journals.org
DOI: 10.1530/ERC-14-0088

Published by Bioscientifica Ltd.